

A means to make an Extremely Bright Entangled Source

Remi Cornwall

University of London Alumni Society, Malet Street, London WC1E 7HU
<http://webspace.qmul.ac.uk/rocornwall> <http://ulondon.academia.edu/RemiCornwall>

Abstract

This paper discusses a means of making an extremely bright path entangled source. An initial laser source is preferred but any source of light: LED, sub-critical laser, coherent or thermal can be used. The light is dimmed by a beam expander until the relative number of $|1\rangle$ or $|2\rangle$ photons increases compared to higher photon states. The expanded beam is then passed through a 1:1 beamsplitter to generate path entanglement on the $|1\rangle$ and $|2\rangle$ photons. A further stage of “purification” can remove the non-entangled higher states by passing the output beams from the beamsplitter through one another, such that the correlated entangled photon electrical fields cancel in some region. In the said region, the uncorrelated non-entangled fields can be Faraday rotated and then absorbed by a polariser. The entangled photons pass through the region without rotation and attenuation. The output from the device then has copious quantities of 1 and 2 photon path entangled suitable for use in telecommunications engineering, secure transmission of data and quantum metrology. The wide beams can be beam-contracted to a thin bright beam and will keep the path entanglement of individual photons, as photons are bosons and so don't interact, furthermore, all operations are unitary and linear, as by Maxwell's equations.

Keywords: Path Entanglement, Non-heralded, Bright Entangled Source, Entanglement Purification

1. Introduction

Entangled photons can be generated by a variety of means: spontaneous parametric down-conversion in non-linear material[1], radiative decay of electron hole pairs in a quantum dot[2-4] or energy-time entanglement from ions in potential traps[5].

An example of the first case, figure 1 shows the spatial layout of the single photon down-conversion system, where a high frequency laser source is incident on a crystal. The majority of the pumping high frequency radiation passes through the crystal (some $10^{12}:1$) and various non-linear processes occur producing uncorrelated beams of different frequencies. Most interesting is the process that leads to down conversion to photons of half the energy and correlation/entanglement. At the intersection of the two middle cones one finds with a ratio of some 1:10,000, entangled photon pairs occasionally created by spontaneous emission and constrained by energy and momentum conservation. Higher powered pumping of the crystal generates more entangled photons though the ratio suffers. Cryogenic temperature can boost the ratio of the desirable entangled photons to unentangled. Obviously physical filtering by restricting most of the gathered photons to the intersection points (we can also use colour filters) increases our chances of recovering the entangled photons.

In this paper will we present a different method of generation, path entanglement and improving the ratio of entangled to unentangled ratio by using the

sine-qua-non of entangled systems – their correlation.

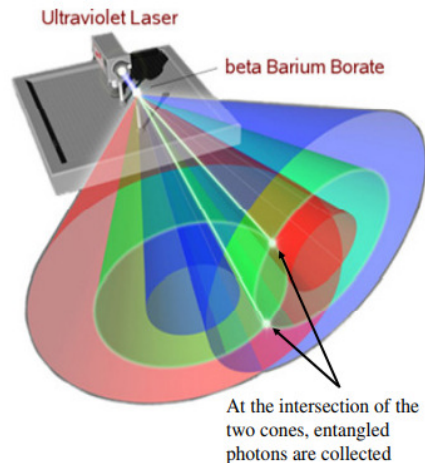


Image copyright of the European Space Agency

Figure 1 – Entanglement by down conversion

2. The generation of path entanglement

The basic operation of mapping the creation-annihilation operators in the Heisenberg representation at the input ports of a beamsplitter is discussed in many places[7-9]. For a 1:1 splitter, the basic creation operation of a single photon incident on one port is this:

$$\begin{pmatrix} \hat{a} \\ \hat{b} \end{pmatrix} \rightarrow \frac{1}{\sqrt{2}} \begin{pmatrix} 1 & 1 \\ 1 & -1 \end{pmatrix} \begin{pmatrix} \hat{c} \\ \hat{d} \end{pmatrix} \quad \text{eqn. 1}$$

Such that,

$$\hat{a}^\dagger \rightarrow \frac{\hat{c}^\dagger + \hat{d}^\dagger}{\sqrt{2}} \quad \hat{b}^\dagger \rightarrow \frac{\hat{c}^\dagger - \hat{d}^\dagger}{\sqrt{2}} \quad \text{eqn. 2}$$

Then a single photon created/incident at the input port maps to the output thus:

$$\begin{aligned} \hat{a}|0\rangle_a|0\rangle_b &= |1\rangle_a|0\rangle_b \rightarrow \frac{1}{\sqrt{2}}(\hat{c}^\dagger + \hat{d}^\dagger)|0\rangle_c|0\rangle_d \\ \Rightarrow \psi_{out} &= \frac{1}{\sqrt{2}}|1\rangle_c|0\rangle_d + \frac{1}{\sqrt{2}}|0\rangle_c|1\rangle_d \end{aligned} \quad \text{eqn. 3}$$

Which is path entangled. For two identical photons (the Hong-Ou-Mandel effect[10]), this can occur:

$$\begin{aligned} \hat{a}\hat{b}|0\rangle_a|0\rangle_b &= |1\rangle_a|1\rangle_b \\ \rightarrow \frac{1}{2}(\hat{c}^\dagger + \hat{d}^\dagger)(\hat{c}^\dagger - \hat{d}^\dagger)|0\rangle_c|0\rangle_d & \quad \text{eqn. 4} \\ \Rightarrow \psi_{out} &= \frac{1}{\sqrt{2}}|2\rangle_c|0\rangle_d + \frac{1}{\sqrt{2}}|0\rangle_c|2\rangle_d \end{aligned}$$

This is path entangled too. McDonald-Wang[9] cover the other scenarios for two photon input, such as two photons at one port.

Input	Output (N_1, N_2)		
$ n_1, n_2\rangle$	(0, 2)	(1, 1)	(2, 0)
$\rightarrow 2, 0\rangle$	$\frac{1}{4}$	$\frac{1}{2}$	$\frac{1}{4}$
$ 1, 1\rangle$	$\frac{1}{2}$	0	$\frac{1}{2}$
$\rightarrow 0, 2\rangle$	$\frac{1}{4}$	$\frac{1}{2}$	$\frac{1}{4}$

Figure 2 – Two-photon entanglement

Higher photon numbers scenarios are covered by them. For instance they present these two tables for the input of three or four photons:

Input	Output (N_1, N_2)			
$ n_1, n_2\rangle$	(0, 3)	(1, 2)	(2, 1)	(3, 0)
$\rightarrow 3, 0\rangle$	$\frac{1}{8}$	$\frac{3}{8}$	$\frac{3}{8}$	$\frac{1}{8}$
$ 2, 1\rangle$	$\frac{3}{8}$	$\frac{1}{8}$	$\frac{1}{8}$	$\frac{1}{8}$
$ 1, 2\rangle$	$\frac{3}{8}$	$\frac{1}{8}$	$\frac{1}{8}$	$\frac{1}{8}$
$\rightarrow 0, 3\rangle$	$\frac{1}{8}$	$\frac{3}{8}$	$\frac{3}{8}$	$\frac{1}{8}$

Figure 3 – Three photons input

Input $ n_1, n_2\rangle$	Output (N_1, N_2)				
	(0, 4)	(1, 3)	(2, 2)	(3, 1)	(4, 0)
$\rightarrow 4, 0\rangle$	$\frac{1}{16}$	$\frac{1}{4}$	$\frac{3}{8}$	$\frac{1}{4}$	$\frac{1}{16}$
$ 3, 1\rangle$	$\frac{1}{4}$	$\frac{1}{4}$	0	$\frac{1}{4}$	$\frac{1}{4}$
$ 2, 2\rangle$	$\frac{3}{8}$	0	$\frac{1}{4}$	0	$\frac{3}{8}$
$ 1, 3\rangle$	$\frac{1}{4}$	$\frac{1}{4}$	0	$\frac{1}{4}$	$\frac{1}{4}$
$\rightarrow 0, 4\rangle$	$\frac{1}{16}$	$\frac{1}{4}$	$\frac{3}{8}$	$\frac{1}{4}$	$\frac{1}{16}$

Figure 4 – Four photons input

Clearly the outputs are entangled by the constraint of particle count. We cannot write, factorise and render the outputs for the 3 or 4-photon case as independent (and so not *entangled*). The conditions where the total count of photons is not three are forbidden, so this factorisation is not permitted:

$$(|0\rangle_c + |1\rangle_c + |2\rangle_c + |3\rangle_c) \otimes (|0\rangle_d + |1\rangle_d + |2\rangle_d + |3\rangle_d)$$

However, through the essentially binomial processing of input creation operators on one port of the splitter,

$$(\hat{c}^\dagger + \hat{d}^\dagger)^N \text{ or } (\hat{c}^\dagger - \hat{d}^\dagger)^N$$

Or both ports,

$$(\hat{c}^\dagger + \hat{d}^\dagger)^N (\hat{c}^\dagger - \hat{d}^\dagger)^M$$

One can see each term in the expansion (for the 1:1 splitter) is:

$$\frac{1}{2^{n-k}} \frac{1}{2^k} \frac{n!}{k!(n-k)!} |n-k\rangle |k\rangle \quad \text{eqn. 5}$$

Then at large N, the output tends to a symmetrical number of photons in each output port, as the more asymmetrical terms have a small coefficient in front of them. In figure 2 the term $|1\rangle|1\rangle$ begins to “swamp” the $|0\rangle|2\rangle$ or $|2\rangle|0\rangle$ terms which would more easily demonstrate the entanglement; more so in figure 4. At very high photon number, a symmetrical term $|N/2\rangle|N/2\rangle$ would show very little difference at the detector between $|N/2\rangle - 1|N/2+1\rangle$ (and nearby) and the path entanglement is masked. Terms that could easily demonstrate the entanglement such as $|N\rangle|0\rangle$ or $|0\rangle|N\rangle$ have a vanishingly small probability of being measured.

In the limit of very high Fock states with the coherent state[11] $|\alpha\rangle$ and the displacement operator sums lots of high states,

$$\hat{D}(\alpha) = e^{(\alpha\hat{a}^\dagger - \alpha^*\hat{a})} \quad \text{eqn. 6}$$

A beamsplitter generates no path entanglement on incident coherent states of *high photon count*,

$$\begin{aligned} \hat{D}_a(\alpha)|0\rangle_a|0\rangle_b &= |\alpha\rangle_a|0\rangle_b \\ &\rightarrow e^{\left(\alpha\left(\frac{\hat{c}^\dagger + \hat{d}^\dagger}{\sqrt{2}}\right) - \alpha^*\left(\frac{\hat{c}^\dagger + \hat{d}^\dagger}{\sqrt{2}}\right)\right)}|0\rangle_c|0\rangle_d \quad \text{eqn. 7} \\ &\Rightarrow \psi_{out} = \frac{1}{\sqrt{2}}|\alpha\rangle_c|\alpha\rangle_d \end{aligned}$$

Knowing that path entanglement dominates at low photon count, our approach is to dim a coherent source (Poisson statistics[11]), fig. 5 or less preferred, a thermal source (Bose-Einstein statistics[12], fig. 6) to the point that Fock states slightly higher than the $|1\rangle$ or $|2\rangle$ states are present in similar numbers, to avoid the “swamping” of unentangled states at the output of the beam-splitter.

The coherent state is Poisson distributed:

$$|\alpha\rangle = e^{-\frac{|\alpha|^2}{2}} \sum_{n=0}^{\infty} \frac{\alpha^n}{\sqrt{n!}} |n\rangle \quad \text{eqn. 8}$$

This has an average photon number $|\alpha|^2$ and the same variance. Graphed below is the average versus the probability. This illustrates what we say about the relative number of the $|1\rangle$ or $|2\rangle$ states to the slightly higher states. We will see later that we can filter these slightly higher states from the output of the splitter.

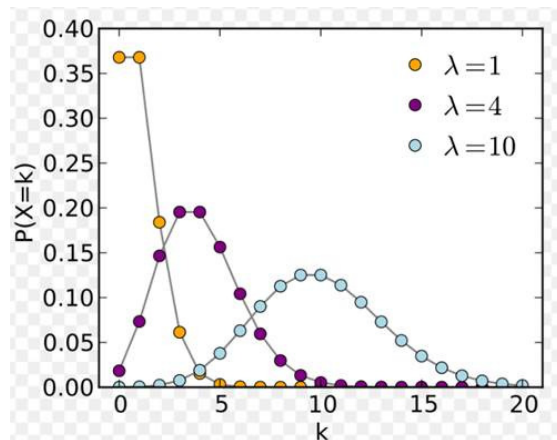


Figure 5 – Poisson distribution, λ is the average

A laser source of high coherence length is practically monochromatic, subject to quantum noise arising from the uncertainty principle. It is of greater use in applications requiring interferometry.

However thermal light (Bose-Einstein distributed) which is *super-Poissonian* distributed (where the variance is greater than the mean) can be dimmed too but with not such a great roll-off of the higher Fock state terms.

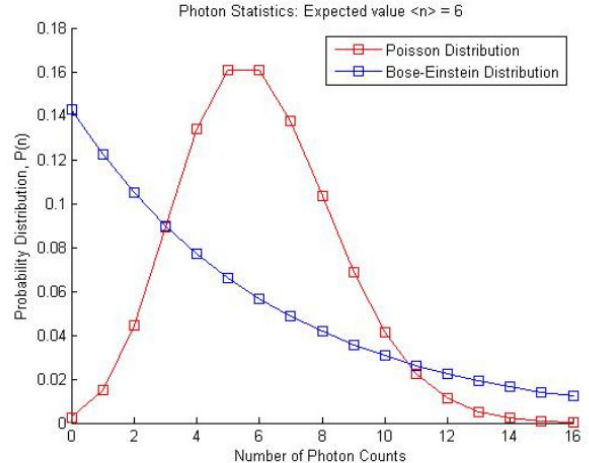


Figure 6 – Comparison of Poisson and Bose-Einstein statistics for an average of six photons

3. Dimming and reconstitution of the beam

The application we envision for this means of producing entanglement is telecoms related, though it may have other uses – such as for ghost imaging and quantum metrology in general with the 2-photon path entangled output. We intend to generate copious quantities of path entangled photons in an intense thin beam (which can be coupled to fibre optic cable) from typically a coherent source. This seems contradictory to the requirement of dimming the input beam and contradictory to eqn. 7.

We argue (figure 7) that there is no such contradiction, as all the operations (beam-expansion/contraction) are linear and unitary from the linearity of the Schrödinger and Maxwell equations and furthermore, photons are bosons and won't interact[13] when put into the same state. The starred points in figure 7 will demonstrate high coincidence counts. The *output beams are in the coherent state with path entanglement*, as the entanglement was done at low photon count (eqn. 3 and eqn. 4), which yields a high proportion of entanglement than if it was done with higher photon numbers (figures 3, 4 and 5).

An estimation of the amount of dimming by beam expansion of a laser beam can be reckoned from the single state volume requirement of a photon.

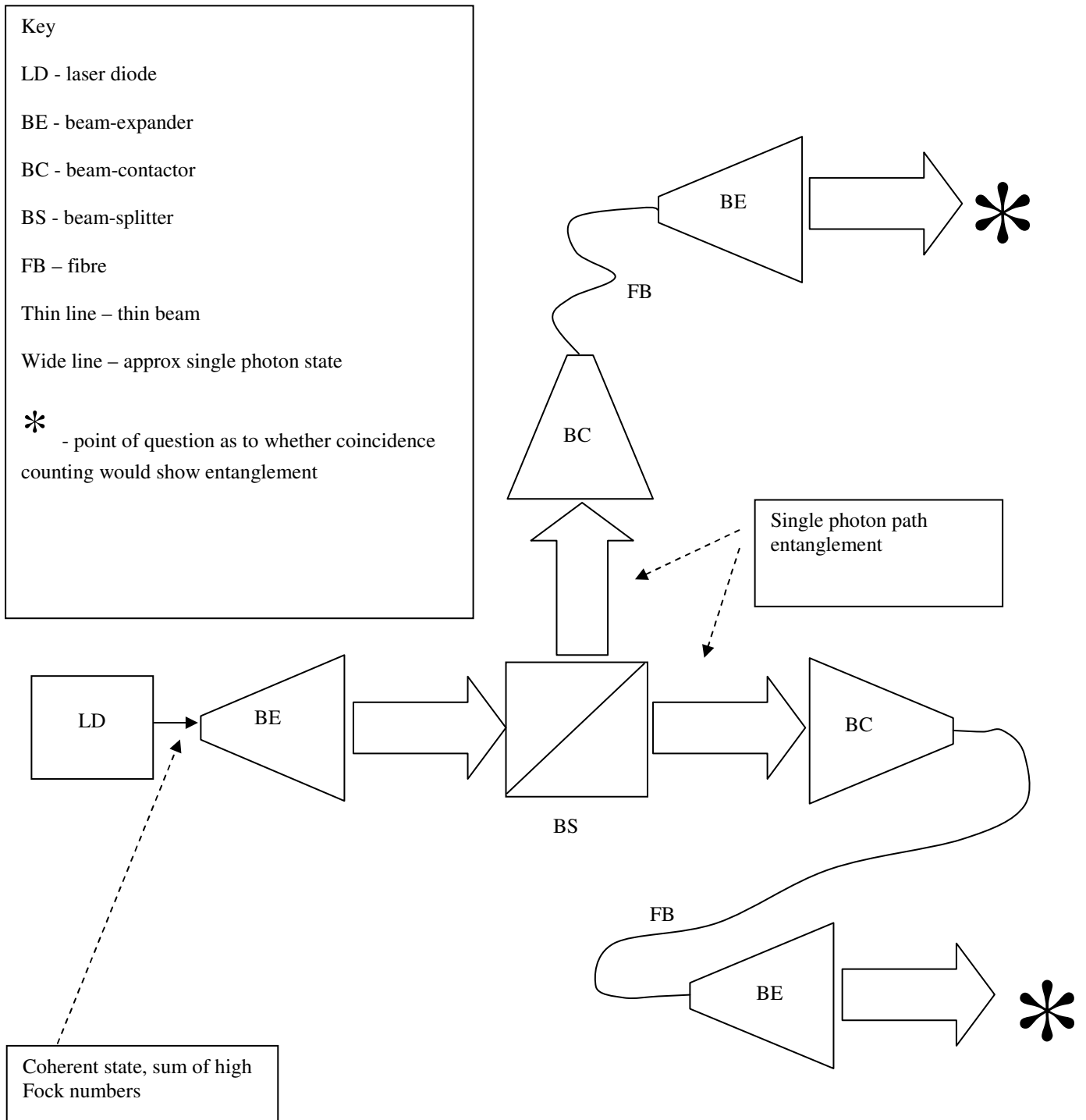


Figure 7 – Dimming by beam-expansion then,
Path entanglement at low photon count then,
Beam-contraction to form an intense, high
photon count, yet path entangled coherent beam

Subject to the uncertainty principle, which sets a limit on the spatial spread and frequency spread of a wavepacket, such that we can model it with a Gaussian envelope (the Gaussian is self-similar under Fourier transformation and the solutions to Maxwell's equations/spin-1 wave equation, it doesn't disperse), we can confine this region to longitudinal extent of 5 wavelengths.

The traverse extent of the photon maybe slightly contentious and moot but we argue that if light is produced in a laser cavity, geometric optics applies and the boundary conditions constrain the propagation of the waves as *rays*. It is then reasonable to say the traverse extent of the single photon is of the order of 5 wavelengths too.

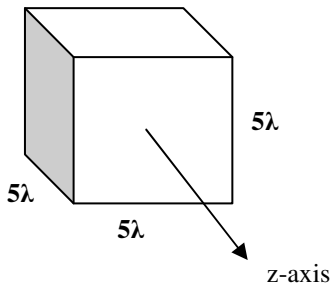


Figure 8 – Ansatz for the space occupied by a single photon

A Gaussian profile laser beam will have similar dimensions and if we know the power, we know the number of photons per second,

$$\text{Photons per second, } n_s = \frac{\text{Power}}{hf} \quad \text{eqn. 9}$$

Through a good approximation (figure 5, the dimming will not alter the statistics), we can figure how wide we need to make the beam so that on average only one photon occupies the volume of one photon. Let us calculate the time of passage of one photon,

$$\text{Time of passage one photon, } \tau = \frac{5\lambda}{c} \quad \text{eqn. 10}$$

So in this time we can reckon how many photons are bunched up in the narrow laser beam from the power levels,

$$\begin{aligned} \text{Bunching} &= n_s \tau \\ &\simeq \frac{5\text{Power}}{hf^2} \end{aligned} \quad \text{eqn. 11}$$

For a 660nm red laser of about 1mW power, we find nearly 40 photons would be counted in the time of passage of one photon. Beam-expansion by

40 times the area of the beam would ensure on average one photon occupying its own volume. We can add an engineering margin on this, of course; the variance of the Poisson distribution is the same as the average and we should factor 3 to 5 times this area to secure a good chance of 1 or 2 photons in the volume (figure 5).

Once the beam has passed through the splitter and been path-entangled, we can contract the beam back down to a fine, intense, beam and couple to fibre, for instance. For reasons already discussed (start of section 3) the path entanglement is preserved, although the beam is coherent and intense.

4. Cleaning up in favour of the low photon number non-entangled photons

It is possible to remove the higher photon state numbers that tend to non-entanglement and the swamping of low photon numbers. Figure 9 shows the schematic whereby: we generate polarised photons (figure 9A) and expand the beam (as previously argued); figure 9B (input from figure 9A) generates the path entanglement, as previously discussed.

Figure 9C takes the output signal and idler pairs (called as such for tradition) from the entanglement process and converges them into a region where their electric fields will overlap. The feature of entanglement is correlation, so the entangled 1-photon states $|1\rangle_c |0\rangle_d + |0\rangle_c |1\rangle_d$ can be made to destructively interfere in this region.

Let us consider what happens with the 2-photon entangled states, McDonald-Wang[9] show a table for this (figure 2). The NOON state is desirable and noting the middle input on the table, this is

obtainable by placing the input laser on both ports of the beam-splitter (figures 7 and 9B); if two single photons are momentarily present on the inputs, this can be achieved. However two photon input will generate the less useful

$|2\rangle|0\rangle + |1\rangle|1\rangle + |0\rangle|2\rangle$ state, which will slip through the scheme in figure 9C, as will other symmetric numbered output photon states, $|3\rangle|3\rangle, |4\rangle|4\rangle$ etc. However, the Poisson distribution (fig. 5) shows the contribution of higher Fock states greater than two precipitously falling. Given this it is better to utilise both ports in figures 7 and 9B.

Unsymmetrical output photon states $|1\rangle|2\rangle, |2\rangle|1\rangle, |1\rangle|3\rangle, |3\rangle|1\rangle$, etc. will be culled by figure 9C scheme, as they present a net electrical field. This is coupled with the fall in higher Fock states by the dimming process.

Figure 9 - Key

LD - laser diode	PLR - polariser	PBS - polarising beam-splitter
BE - beam-expander	BS - beam-splitter	FR - Faraday Rotator
BC - beam-contactor	FB - fibre	

Fig. 9A

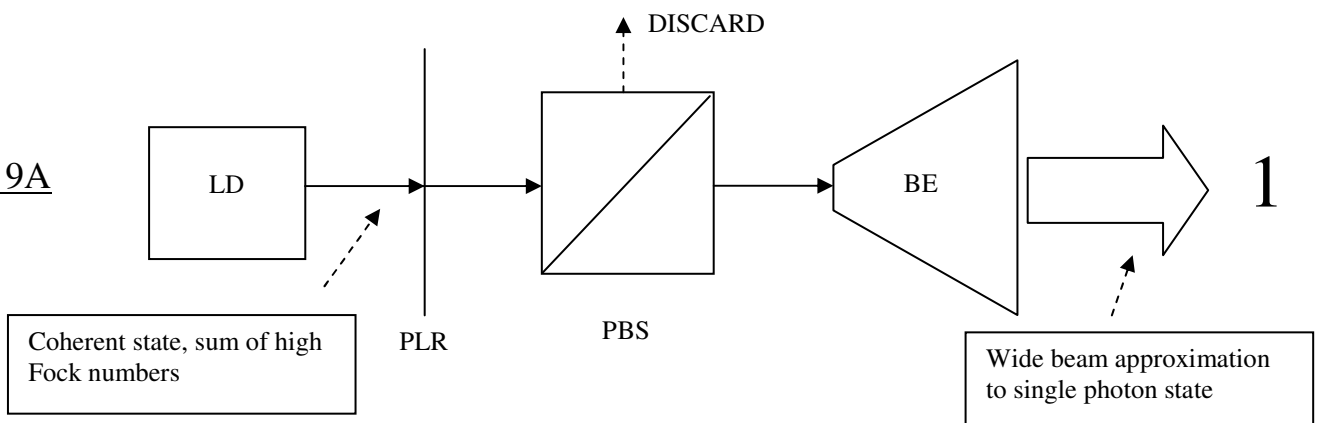


Fig. 9B

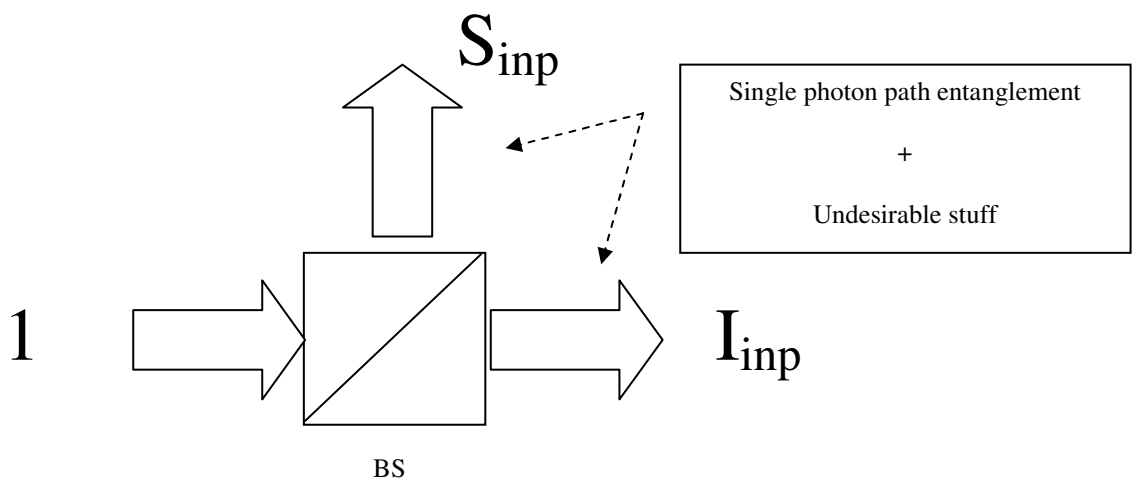


Fig. 9C

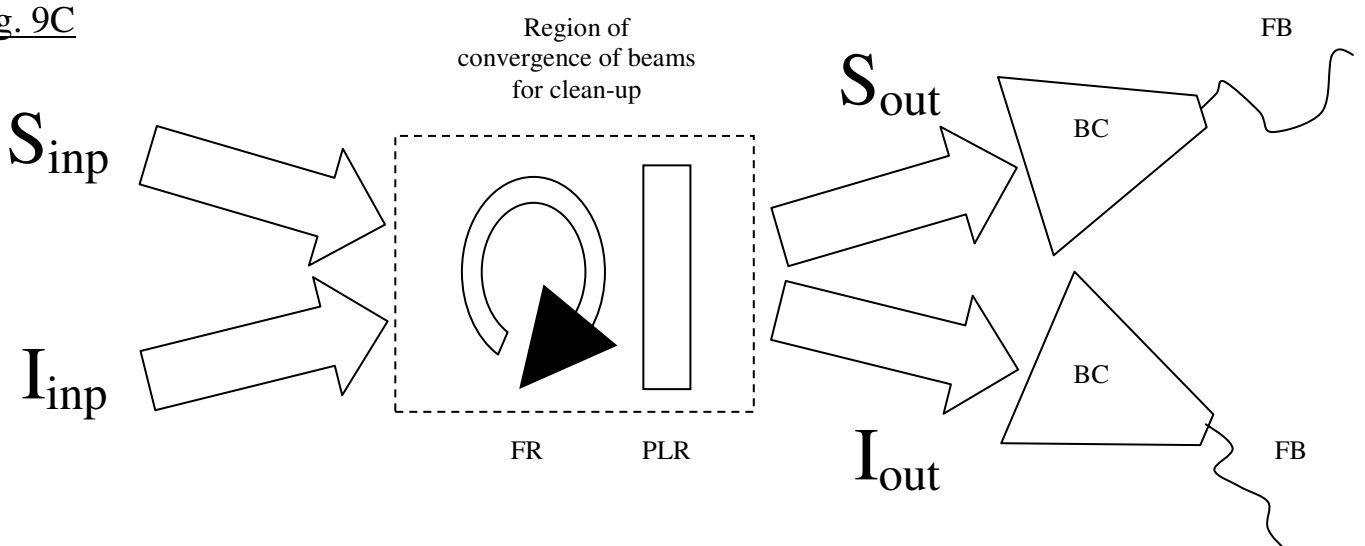


Figure 9C shows the outputs contracted down to a fibre that sends a very bright light, that when expanded at the far end of the fibre, will contain copiously high numbers of $|1\rangle|0\rangle + |0\rangle|1\rangle$ entangled photons, with $|2\rangle|0\rangle + |0\rangle|2\rangle$ in the ratio of some $(0.2/0.35)^2$ (figure 5), approximately 0.33, by two beam-expansions and then $|1\rangle|1\rangle$ at relatively half that, so approximately 0.16.

$ 1\rangle 0\rangle + 0\rangle 1\rangle$	$ 2\rangle 0\rangle + 0\rangle 2\rangle$	$ 1\rangle 1\rangle$
Copious	Ratio 0.33	Ratio 0.16

5. Applications

This method generates the $|20,02\rangle$ state, which although not particularly great by today's standards (up to $|50,05\rangle$ [15-16]), is at least produced in copious quantities (trillions of trillions quantities at least) and relatively free or completely free of undesirable other states (un-entangled or symmetrical states $|n,n\rangle$) but with a relatively higher amount of the $|10,01\rangle$. This has application to quantum metrology and ghost-state imaging.

Our intended application is secure communication over telecoms fibre (figure 10A/B after references). This utilises single photon self-interference, such that if a measurement is performed ("Alice"), the receiver's interference pattern ("Bob") will be destroyed. If the beam-expansion technique and filtering discussed in this paper is used, then classical data can be sent over a quantum channel very securely and robustly by sending trillions of path-entangled photons to represent one bit. It may be possible not to use the filtering scheme of figure 9; other undesired photon combinations would just contribute a "bias" signal at the destructive interference output with a hefty data signal riding it, anyway.

References

1. Burnham D. C., Weinberg D. L., *Observation of simultaneity in parametric production of optical photon pairs*. Phys. Rev. Lett., 1970. **25**(84).
2. Young, R.J., *Improved fidelity of triggered entangled photons from single quantum dots*. N. J. Phys., 2006. **8**(29).
3. Akopian, N. et al., *Entangled photon pairs from semiconductor quantum dots*. Phys. Rev. Lett., 2006. **96**: p. 130501–130504.
4. Muller, A., Fang, W., Lawall, J. & Solomon, G. S., *Creating polarization-entangled photon pairs from a semiconductor quantum dot using the optical Stark effect*. Phys. Rev. Lett., 2009. **103**.
5. Franson, J.D., *Bell Inequality for Position and Time*. Phys. Rev. Lett., 1989. **62**(19).
6. Dousse, A.; Suffczynski, J.; et al, *Ultrabright source of entangled photon pairs*. Nature, 2010. **466**: p. 217-220.
7. Gerry, Christopher; Knight, *Introductory Quantum Optics*. 2004: CUP.
8. Ralph, Hans-A Bachor; Timothy C., *A Guide to Experiments in Quantum Optics*. 2004: Wiley-VCH.
9. Kirk T. McDonald, Lijun J. Wang, *Bunching of Photons When Two Beams Pass Through a Beamsplitter*. 2003; Available from: <https://arxiv.org/abs/quant-ph/0312032>.
10. Mandel, C. K. Hong; Z. Y. Ou & L, *Measurement of subpicosecond time intervals between two photons by interference*. Phys. Rev. Lett., 1987. **59**(18).
11. Glauber, R., *Coherent and Incoherent States of the Radiation Field*. Phys. Rev. Lett., 1963. **10**(84).
12. Landau, Lifshitz., *A Course in Theoretical Physics: Statistical Physics*. Vol. Vol. 5. 1996: Butterworth Heinemann.
13. Zurek, W.H., *Decoherence and the Transition from Quantum to Classical*. Los Alamos Science, 2002. **27**.
14. Feynman, Leighton, Sands, *The Feynman Lectures on Physics*. Addison-Wesley, Reading, Massachusetts. Vol. 1, 2, 3. 1989.
15. A. E. B. Nielsen, K. Molmer, *Conditional generation of path-entangled optical NOON states*. Phys. Rev. A. 75, 2007.
16. Afek Itai, Oron Ambar, Yaron Silberberg, *High NOON State by Mixing Quantum and Classical Light*. Science, 2010. **328**.

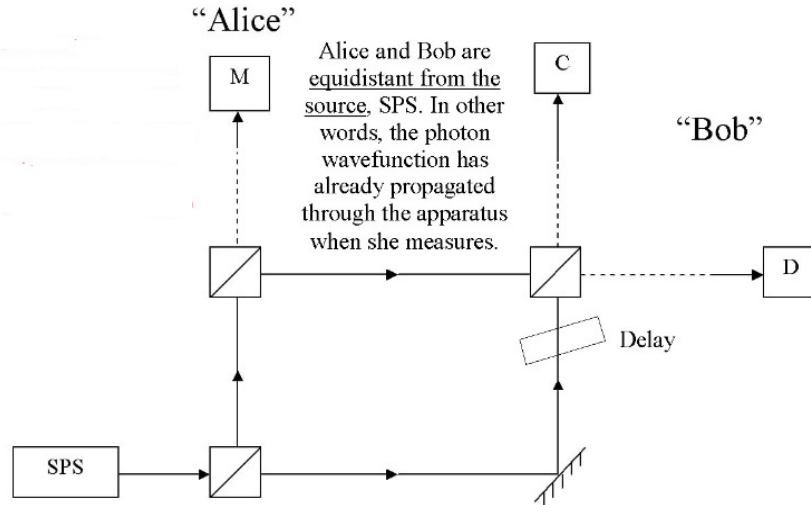


Figure 10A – Secure communication

This is the fundamental law of Quantum Mechanics:-

If the paths can be distinguished then add probabilities

else if the paths can't be, then add amplitudes before calculating probabilities

Thus when Alice measures, both of Bob's paths to his detectors become distinguishable.

Alice sends	Bob receives
Binary 0: No measurement	Binary 0: Min signal, destructive interference from pure state at D
Binary 1: Measurement	Binary 1: Max signal from mixed state at D

$$\begin{aligned}
 P(\text{Bob few photons, binary 0} | \text{Alice no measurement}) &= \left| \frac{i}{\sqrt{2}} \right|^2 + \left| \frac{e^{i\theta}}{\sqrt{4}} \right|^2 + 2 \left| \frac{i}{\sqrt{2}} \right| \left| \frac{e^{i\theta}}{\sqrt{4}} \right| \cos \theta \\
 &= 0.5 + 0.25 + \frac{1}{\sqrt{2}} \cos \theta \\
 &\approx 0.75 \pm 0.707 \cos \theta \\
 &\approx 0.043 \text{ minimum}
 \end{aligned}$$

$$\begin{aligned}
 P(\text{Bob lots of photons, binary 1} | \text{Alice measurement}) &= \left| \frac{i}{\sqrt{2}} \right|^2 + \left| \frac{i}{\sqrt{4}} \right|^2 \\
 &= 0.5 + 0.25 \\
 &= 0.75
 \end{aligned}$$

Figure 10B – Measurement/No-measurement protocol